Available online at www.sciencedirect.com
SCIENCE DIRECT®
Journal of Hydrology 284 (2003) 57–76
Journal of Hydrology
www.elsevier.com/locate/jhydrol

Application of two hydrologic models with different runoff mechanisms to a hillslope dominated watershed in the northeastern US: a comparison of HSPF and SMR

Mark S. Johnson[a,1], William F. Coon[b], Vishal K. Mehta[a], Tammo S. Steenhuis[a,*], Erin S. Brooks[c], Jan Boll[c]

[a]*Department of Biological and Environmental Engineering, Cornell University, 226 Riley-Robb Hall, Ithaca, NY 14853 5701, USA*
[b]*US Geological Survey, 30 Brown Road, Ithaca, NY 14850, USA*
[c]*Department of Biological and Agricultural Engineering, University of Idaho, Moscow, ID 83844, USA*

Received 29 May 2002; accepted 9 July 2003

Abstract

Differences in the simulation of hydrologic processes by watershed models directly affect the accuracy of results. Surface runoff generation can be simulated as either: (1) infiltration-excess (or Hortonian) overland flow, or (2) saturation-excess overland flow. This study compared the Hydrological Simulation Program—FORTRAN (HSPF) and the Soil Moisture Routing (SMR) models, each representing one of these mechanisms. These two models were applied to a 102 km^2 watershed in the upper part of the Irondequoit Creek basin in central New York State over a seven-year simulation period. The models differed in both the complexity of simulating snowmelt and baseflow processes as well as the detail in which the geographic information was preserved by each model.

Despite their differences in structure and representation of hydrologic processes, the two models simulated streamflow with almost equal accuracy. Since streamflow is an integral response and depends mainly on the watershed water balance, this was not unexpected. Model efficiency values for the seven-year simulation period were 0.67 and 0.65 for SMR and HSPF, respectively. HSPF simulated winter streamflow slightly better than SMR as a result of its complex snowmelt routine, whereas SMR simulated summer flows better than HSPF as a result of its runoff and baseflow processes.

An important difference between model results was the ability to predict the spatial distribution of soil moisture content. HSPF aggregates soil moisture content, which is generally related to a specific pervious land unit across the entire watershed, whereas SMR predictions of moisture content distribution are geographically specific and matched field observations reasonably well. Important is that the saturated area was predicted well by SMR and confirmed the validity of using saturation-excess mechanisms for this hillslope dominated watershed.

Keywords: Distributed modeling; Saturation excess; Infiltration excess; Runoff mechanisms

* Corresponding author. Tel.: +1-607-255-2489; fax: +1-607-255-4080.
E-mail address: tss1@cornell.edu (T.S. Steenhuis).
[1] Present address: Department of Crop and Soil Sciences, Cornell University, Ithaca, NY 14853, USA.

0022-1694/$ - see front matter © 2003 Elsevier B.V. All rights reserved.
doi:10.1016/j.jhydrol.2003.07.005

1. Introduction

Computer simulation models of watershed hydrology are widely used to examine watershed-scale processes and to evaluate the hydrologic effect of various management scenarios. The use of watershed models is increasing in response to growing demands for improved environmental quality and is evolving as a tool for development of environmental regulations, such as Total Maximum Daily Loads (TMDLs). The complexity of watershed models is also increasing with recent advances in computer technology, which allow simulation of the myriad of hydrologic conditions and processes that occur in hydrologic systems.

Watershed models can be categorized according to their runoff-generating mechanism, which can be either: (1) infiltration-excess overland flow (or Hortonian overland flow), (2) saturation-excess overland flow, (3) an empirical relation, or (4) a combination of (1), (2), and (3). Infiltration-excess overland flow is generated when the precipitation rate exceeds the infiltration capacity of the soil or land surface, and can be a dominant process in urbanized or otherwise disturbed areas, as well as in areas that typically receive high intensity precipitation and that have a low permeable crust at the soil surface. Saturation-excess overland flow is generated when the soil becomes saturated to the extent that additional precipitation cannot infiltrate. Saturation-prone areas are primarily those with a high water table and shallow soils that provide little additional storage for water (Dunne, 1978). Empirical relations between watershed factors are statistically derived and have little physical basis.

Few studies have compared the results of differing watershed models applied to the same catchment; summaries of much of the relevant literature are given by Perrin et al. (2001), Refsgaard and Knudsen (1996), and Michaud and Sorooshian (1994). Comparative studies are needed to assess the applicability and limitations of watershed models, but the studies to date have tended to focus either on model performance (World Meteorological Organization, 1975, 1986, 1992), or on differences in model structure (such as conceptual models vs. distributed-data models). Perrin et al. (2001) state that comparative studies tend to report differences that are not significant enough to be consistently interpreted as evidence of model quality. Franchini and Pacciani (1991) conclude that despite the wide range of structural complexity among the models compared, the results are similar and equally valid. In contrast, Gan et al. (1997) report that significant differences among results from differing models applied to a common watershed were primarily due to differences in the models' runoff-generating mechanisms and concluded that a variable-source hydrology model consistently produced better results than the other models tested.

Two watershed models, the Hydrological Simulation Program—FORTRAN (HSPF) model, which uses an infiltration-excess mechanism to simulate overland flow, and the Soil Moisture Routing (SMR) model, which uses a saturation-excess overland flow mechanism, were compared in their abilities to simulate runoff from a 102 km^2 watershed in the upper part of the Irondequoit Creek basin in central New York State over a seven-year simulation period. HSPF has been used to simulate: (1) a wide variety of hydrologic conditions (Srinivasan et al., 1998; Zarriello and Ries, 2000), (2) transport of various non-point source pollutants, including contaminated sediment (Fontaine and Jacomino, 1997) and pesticides (Laroche et al., 1996), and (3) land use management and flood control scenarios (Donigian et al., 1997). SMR, developed by us, has been used in a limited number of cases as a water quality management tool for rural watersheds (Boll et al., 1998), and appears to effectively simulate variable-source-area hydrology (Frankenberger et al., 1999; Walter et al., 2000). There are many differences between these two models, but those that affect the models' treatment of hydrologic processes, which are considered important in the study area, are emphasized.

1.1. Overview of HSPF and SMR

HSPF is based upon the original Stanford Watershed Model IV (Crawford and Linsley, 1966) and is a consolidation of three previously developed models: (1) Agricultural Runoff Management Model (ARM) (Donigian and Davis, 1978), (2) Non-point Source Runoff Model (NPS) (Donigian and Crawford, 1976), and (3) Hydrological Simulation Program (HSP), including HSP Quality (Hydrocomp, Inc., 1977;

Donigian and Huber, 1991; Donigian et al., 1995). In addition, HSPF is embedded in the US Environmental Protection Agency's water quality assessment tool, BASINS (Lahlou et al., 1998). An extensive description of HSPF is given in Bicknell et al. (1997).

1.1.1. HSPF model

HSPF is a semi-distributed, conceptual model (Fig. 1) that combines spatially distributed physical attributes into hydrologic response units (HRUs), each of which, in response to meteorological inputs (such as precipitation, potential evapotranspiration, and temperature) and storage-capacity factors (such as interception, surface retention, and soil-moisture storage), is assumed to behave in an uniform manner. Surface runoff is simulated primarily as an infiltration-excess process. The outputs (as surface flow, interflow, and groundwater flow) from each HRU represent the average response of the HRU to precipitation and are routed to a stream channel. Flow is routed downstream from reach to reach by storage routing (kinematic wave) methods.

HSPF allows modelers to emphasize the hydrologic processes that are dominant in a watershed by specifying the major characteristics used to define HRUs, such as soil type or land use, and by adjusting parameter values during calibration. Although selection of parameter values that reflect watershed-specific physical processes can improve model calibration, estimation of actual parameter values from physical measurements is either difficult or impossible (Jacomino and Fields, 1997). Therefore, optimum parameter values are generally obtained through the calibration process. Calibration of the model entails adjustment of pertinent parameters to minimize the differences between simulated and observed streamflow characteristics, including annual runoff, storm volume and peak flows, volume of high

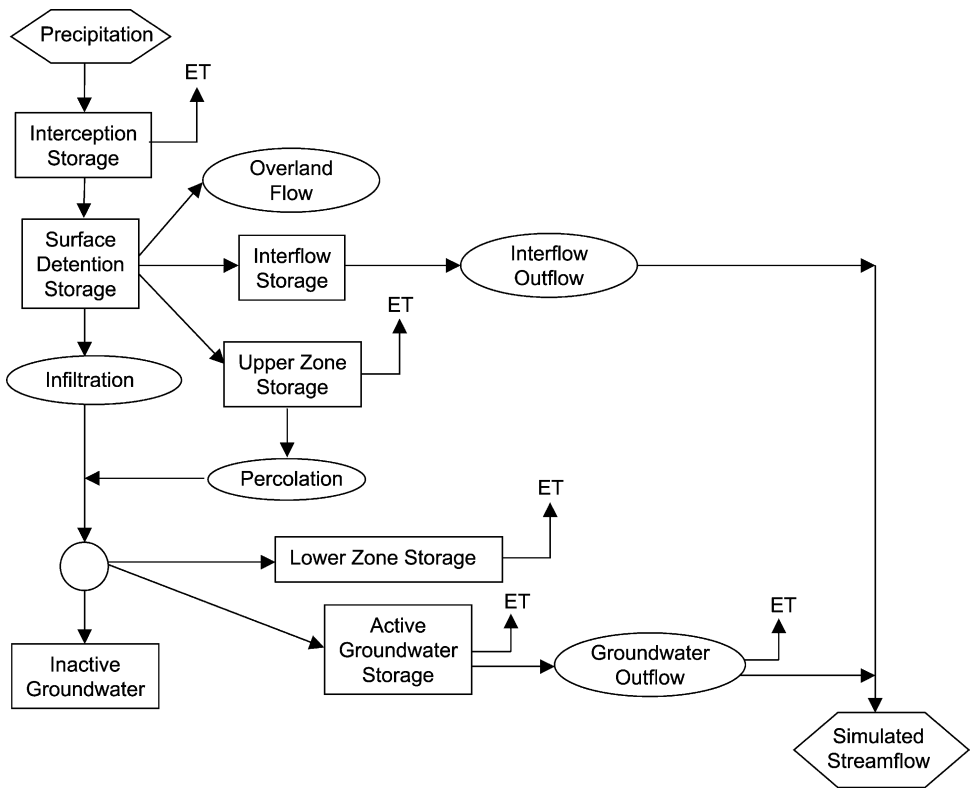

Fig. 1. HSPF conceptual hydrologic model.

and low flow periods, baseflow recession rate, and summer and winter flow volumes. Parameters that generally have a large effect on runoff volume and timing control the processes that simulate infiltration, interflow, surface and soil moisture storage and losses through evapotranspiration, and interflow and groundwater recession rates.

1.1.2. SMR model

SMR is a raster GIS-based, physically distributed watershed model (Fig. 2) that incorporates saturation excess as the primary runoff-generating mechanism (Zollweg et al., 1996; Frankenberger et al., 1999). Physically based equations are applied to each grid cell at each time step. Parameters used in SMR are derived from soil survey and remotely sensed data, and are supplemented with field data where possible. The soil survey data can be applied to as many as four soil layers without modification.

A water balance for each time step is calculated from moisture inputs, subsurface lateral flow, deep percolation, and runoff. Runoff is generated when rainfall exceeds the storage capacity of a grid cell. At the beginning of each time step, precipitation and snowmelt inputs are added to the soil moisture volume of the soil profile of each grid cell. This volume is then distributed among the layers in proportion to each layer's thickness and water-holding capacity. If micropore storage is satisfied for all layers, the remaining moisture begins filling the soil layers to saturation, beginning with the deepest layer and proceeding upwards to successive layers.

Both the physical representation and the distributed nature of SMR permits assessment of a watershed's response to precipitation on both integrated and distributed levels. Integration of surface runoff over the watershed at each time step allows comparison with observed streamflow. Unlike HSPF, distribution of SMR results, such as soil moisture content (Frankenberger et al., 1999 and present study) and water table depths (Boll et al., 1998), can be evaluated at a grid cell scale through a variety of analytical methods to compare predicted results with observed values.

1.2. Hydrologic processes as represented by HSPF and SMR

1.2.1. Runoff generation

HSPF is primarily an infiltration-excess model that separates moisture inputs (precipitation and snowmelt) into infiltrating and non-infiltrating fractions according to three conceptual parameters: a surface storage capacity value (UZSN), an interflow–inflow index (INTFW), and an infiltration-capacity index (INFILT) that decreases as soil moisture increases.

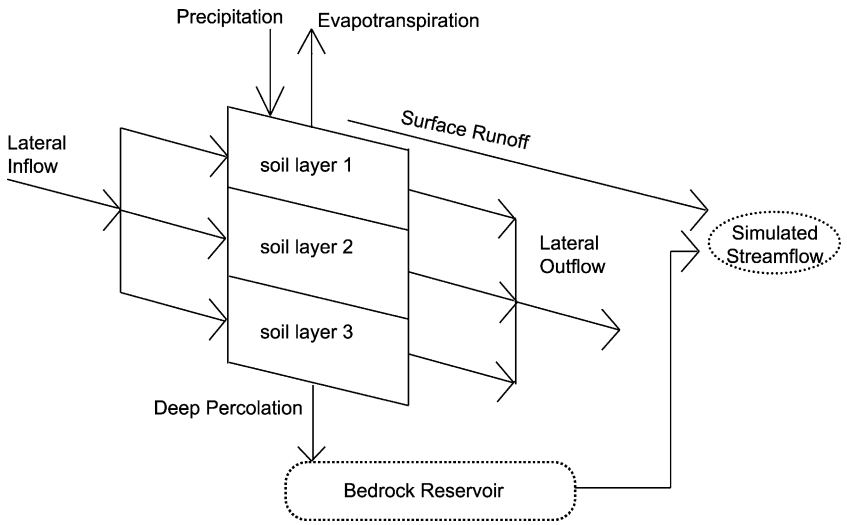

Fig. 2. SMR conceptual hydrological model.

Saturation-excess overland flow can be simulated by adjusting the exponent used in the infiltration equation (parameter INFEXP, Berris, 1995, p. 12), as well as the infiltration-capacity index and soil-moisture storage parameters. In this way, overland flow can be inhibited during dry seasons, but substantial runoff can be generated during wet periods. The accuracy of saturation-excess flow simulation by HSPF depends on careful delineation of those areas in the watershed where saturation-excess flow might be a dominant flow mechanism, but in almost all applications of HSPF, modelers use the default value for INFEXP (Donigian et al., 1999) and allow infiltration-excess overland flow to be the dominant runoff-generating mechanism. Overland flow is treated as a turbulent flow process and is simulated by the Chezy–Manning equation and average values of the surface roughness, length, and slope for the overland flow plane of each HRU.

SMR generates runoff in response to saturation excess—the moisture in excess of soil-moisture storage capacity after moisture is routed from each grid cell laterally by subsurface lateral flow, and vertically by percolation and evapotranspiration from the root zone. The excess moisture from each cell is aggregated (summed) as streamflow at the outlet of the simulated watershed on a daily basis.

1.2.2. Subsurface lateral flow

Subsurface lateral flow has a substantial effect on stormflow hydrographs, particularly in areas where vertical percolation is retarded by bedrock or a shallow, poorly permeable soil layer. Subsurface lateral flow is termed interflow–outflow (IFWO) in HSPF. It is calculated on the basis of a linear relation between the conceptual interflow-storage volume and lateral flow as a function of the interflow-recession coefficient (IRC). IRC, which is the ratio of the present rate of IFWO to the value 24 h earlier, can be input on a monthly basis to allow for annual variations in soil-moisture and the timing of IFWO (Bicknell et al., 1997).

Subsurface lateral flow is computed in SMR by Darcy's Law, which is applied on the assumption that the hydraulic gradient is parallel to soil surface topography. At each time step, the following equation (Boll et al., 1998) is applied to each grid cell:

$$Q_{\text{in,out}} = \sum_{j=1}^{n} wK(\theta_j)D_j\beta \tag{1}$$

where $Q_{\text{in,out}}$ =lateral flow into or out of each cell, n = number of soil layers for soil type of each cell, w = width of each cell, $K(\theta_j)$ = effective (lateral) hydraulic conductivity of soil layer j, D = thickness of the soil layer, and β = slope of the land surface. The effective (lateral) hydraulic conductivity, $K(\theta_j)$, which is used to compute subsurface lateral flow through the vadose zone, incorporates a dual-porosity and dual-permeability approach (Jarvis and Larsson, 2001), wherein separate equations are applied to each of two subsurface flow regimes: preferential flow through macropores and matrix flow through micropores. The matrix flow uses an exponentially decreasing unsaturated hydraulic conductivity function with moisture content (Kuo et al., 1999). The effective saturated conductivity decreases with depth and was first applied to SMR by Boll et al. (1998) to reflect the assumption of decreasing macroporosity with depth.

1.2.3. Snowfall and snowmelt

HSPF and SMR both use temperature criteria to determine whether precipitation falls as snow or rain. In HSPF, air and dew point temperatures are used to calculate the rain–snow threshold. If the average elevation of an HRU is appreciably different than the elevation of the temperature recording station, then the air temperature can be adjusted. If this adjustment results in a dew point that is higher than air temperature, the dew point will be set equal to the air temperature. In addition to temperature data, HSPF requires a time series of solar radiation and wind velocity to simulate snowmelt through a sequence of routines that computes net radiation exchange on the snow surface, convection of sensible heat from the air, latent heat transfer by condensation, and conduction of heat from the underlying ground to the snowpack. SMR computes snowmelt using a simple temperature index that represents snowmelt as a water balance problem based on empirical relations given in US Army Corps of Engineers (1960). Because the topographic information is preserved, SMR can spatially distribute

the temperature input data using an adiabatic lapse rate (3.5 F/1000 ft or 0.00636 °C/m).

1.2.4. Aquifer recharge

In HSPF, water that infiltrates or percolates from the upper soil zone may enter: (1) lower zone storage as determined by the parameter LZSN, (2) inactive groundwater storage, or (3) active groundwater storage. The fraction of groundwater that enters inactive groundwater is considered lost from the watershed as deep aquifer recharge and is controlled by the parameter DEEPFR; the remainder enters active groundwater storage and is available for discharge to surface channels.

In SMR, aquifer recharge occurs as percolation from the soil profile if micropores are filled. The rate of recharge varies spatially depending upon the composition of the soil substratum. Soil survey information is used to classify each soil substratum (and corresponding grid cells) as either free drainage (e.g. underlain by bedrock) or limited drainage (e.g. underlain by fragipan) (Table 1). A flux of 0.1 mm/day is used for restricted drainage (Boll et al., 1998), whereas the flux through an unrestricted substratum is calculated from analysis of streamflow during low flow periods that are not strongly affected by snowmelt or evapotranspiration. This is further explained in Section 1.2.5.

1.2.5. Aquifer discharge

SMR and HSPF both simulate aquifer discharge as the removal of groundwater from a conceptual, lumped aquifer storage at each time step. HSPF aggregates baseflow for each HRU, whereas SMR aggregates baseflow over the entire watershed.

Table 1
Soil-drainage classification used for the SMR model of the Irondequoit Creek basin, Monroe County, NY (Heffner and Goodman, 1973; Pearson and Cline, 1958)

Description	Percolation class
Free draining	Freely draining
Well drained	Freely draining
Moderate to high permeability	Freely draining
Contains hardpan or fragipan	Limited drainage
Moderately low to low permeability	Limited drainage

HSPF estimates groundwater outflow from active groundwater storage as a function of three parameters: active groundwater storage (AGWS), the active groundwater recession coefficient (AGWRC), and the active groundwater outflow modifier (KVARY), which governs the extent to which aquifer recharge affects aquifer discharge to the stream.

Previous applications of SMR estimated aquifer discharge by calculating a linear reservoir coefficient through an analysis of recessions (Frankenberger et al., 1999). Complexities in the aquifer dynamics of the study area, including deep lateral groundwater flow leaving as underflow and not being measured by the stream-gaging station (Kappel and Young, 1989), prompted a new approach, however. The present application of SMR used an approach patterned on that of TOPMODEL (Beven et al., 1995) to simulate the baseflow contribution to streamflow. A straight line plot of $1/Q$ as a function of time indicates that discharge has an inverse (first-order hyperbolic) relation to time:

$$Q_b^{-1} = Q_o^{-1} + tm^{-1} \quad (2)$$

where Q_b = baseflow at time step, Q_o = drought discharge, t = number of time steps since precipitation, and m = slope of line in the $1/Q$ vs. time plot. Q_o corresponds to the lowest recorded streamflow during the period of record. Beven et al. (1995) states that m can be calculated from recession curves that are not strongly influenced by evapotranspiration or snowmelt processes.

1.2.6. Evapotranspiration

Both models require a times series of potential evapotranspiration (PET) values, which was calculated at each time step through the Penman–Monteith method (DeGaetano et al., 1994). HSPF computes evapotranspiration (ET) as a function of moisture storage and PET, which is adjusted for vegetation cover, and estimates actual ET from the potential demand from five sources (Fig. 1): (1) interception storage, (2) upper-zone storage; that is, some or all the moisture in depressions and near-surface retention, (3) vegetation demand, which is satisfied from lower-zone storage through the parameter LZETP, which can be adjusted monthly to account for seasonal changes in the plant growth stage and soil moisture,

(4) deeply rooted vegetation demand, which is satisfied from active groundwater storage through the parameter AGWETP, and (5) riparian-vegetation demand, which is satisfied by active groundwater outflow as stream baseflow through the parameter BASETP. SMR calculates ET by the Thornthwaite–Mather method (Thornthwaite and Mather, 1955) for each grid cell at each time step as a function of PET, soil moisture content, and a vegetation coefficient based upon Allen (1998).

2. Materials and methods

2.1. Site description

The watershed is located about 20 km southeast of Rochester, NY, and comprises the southern part of the Irondequoit Creek basin upstream from the USGS streamflow monitoring station at Railroad Mills near Fishers, NY (Lat 43°01′40″N, Long 77°28′42″W) (Fig. 3). The study area is representative of the glaciated undulating landscape with shallow soils that is common in the northeastern US. Topography in the rural 101.5 km^2 study area is predominantly gently rolling hills. Land use is mainly open grass/shrub (former pasture and hay fields), forest, agriculture, and rural residential. Average annual precipitation (1991–1998) recorded at the National Weather Service (NWS) station at the Greater Rochester International Airport (about 12 km northwest of the study area) is about 800 mm, including the contribution from an average annual snowfall of about 2.3 m (water content about 230 mm). Mean annual discharge of Irondequoit Creek at Railroad Mills for 1991–1999 was 345 mm (Hornlein et al., 1999).

The watershed contains a glacially scoured bedrock trough in the pre-glacial Irondogenesee River valley. This trough was filled with unconsolidated glacial material during the retreat of the glacier; these materials now form a deep aquifer that underlies a part of the study area (Kappel and Young, 1989). The thickness of unconsolidated material (overburden) above the bedrock surface ranges from 0 m to more than 130 m. Aquifer recharge in the study area results from the infiltration of precipitation on upland glacial sand and silty sand deposits, and from direct runoff from the uplands that infiltrates sandy deposits along some of the tributaries (Kappel and Young, 1989). Groundwater discharges from the watershed as springs in the Railroad Mills area and as seepage to Irondequoit Creek. It also moves northward as underflow through the deep unconsolidated deposits in the preglacial Irondogenesee River valley (Kappel and Young, 1989).

Field observations indicate that saturation-excess runoff is a hydrologic process, at least in some parts of the study area; saturated areas were observed during dry as well as wet periods. The varying spatial extent of the saturated areas over time indicates that they are variable-source areas as defined by Dunne (1978).

2.2. Application of models to study area

Both models were developed from the same data wherever possible. Raster GIS-based maps common to the two models included Digital Elevation Models (DEMs), soils, and land use/land cover maps. The smallest available grid cell size (10 m) was used for development of the models because the fine resolution it provides has been shown to produce more accurate results than a large grid cell size (Kuo et al., 1999).

2.2.1. Input data

The required input data and the preprocessing analyses of the data for the HSPF model differed from those for the SMR model as a result of the structural differences between HSPF and SMR (lumped-parameter, conceptual vs. physically distributed). The following sections explain these differences as they pertain to the DEM, soils, and land use/land cover maps, as well as the meteorological input data.

2.3. Digital elevation model (DEM)

In the HSPF model, a DEM-derived slope map was used to define hydrologic response units (HRUs) by assigning slope to one of two categories—less than 6% and greater than 6%. An average slope value from within each of these categories was used to compute overland flow. The SMR model was based on DEM-derived gradients between neighboring grid cells, which were used to route subsurface lateral flow downhill from cell to cell through multiple flow paths. SMR also used the DEM to obtain a spatially distributed temperature input (by an adiabatic lapse

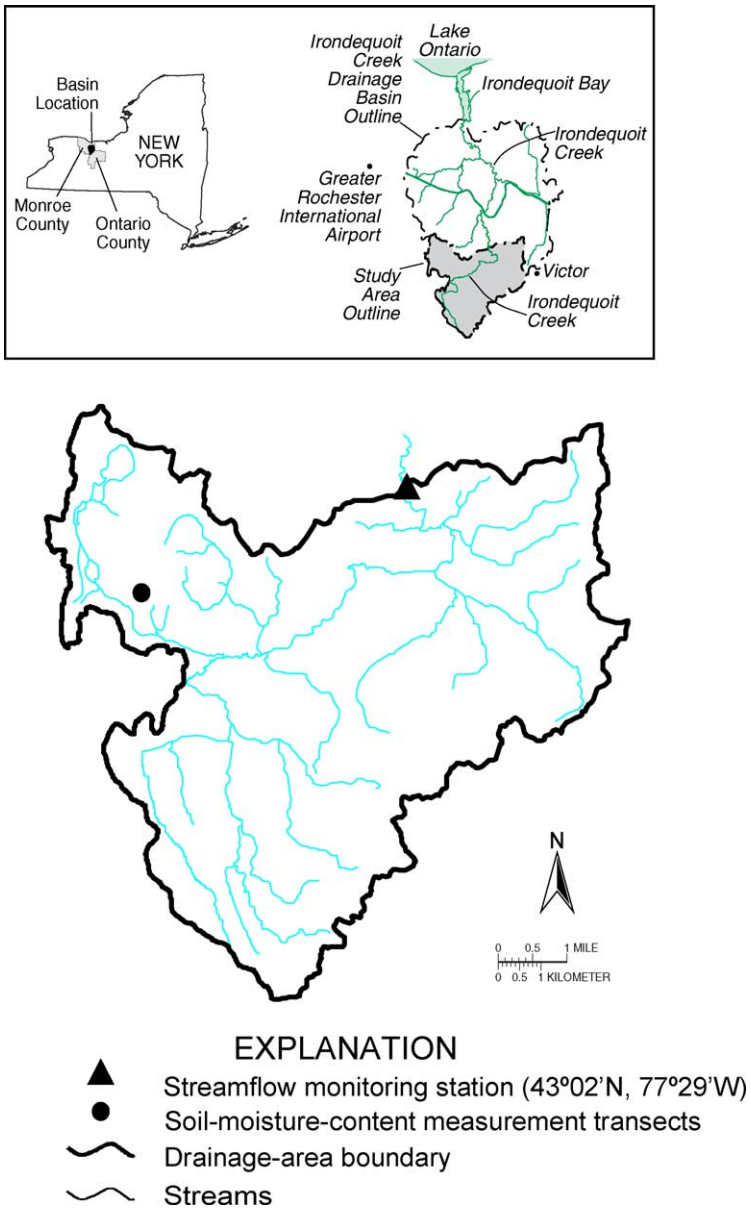

Fig. 3. Location of study area within the Irondequoit Creek basin, Monroe and Ontario Counties, NY.

rate) to determine whether precipitation fell as snow or rain and to calculate snowmelt.

2.4. Soils data

The digital soils map corresponded to the Soil Conservation Service soil surveys of Monroe and Ontario Counties, NY (Pearson and Cline, 1958; Heffner and Goodman, 1973). Soil parameter data were obtained from the Soil Survey Geographic database (SSURGO) for Monroe County, and from the Soils 5 database (EarthInfo, 1993) for Ontario County.

The HSPF model used the soils data to define HRUs. Soils were assigned to one of two categories based on the permeability given for the B horizon

(generally between 25 and 100 cm below the land surface) in the soil surveys. The two categories were: low permeability (less than or equal to 5 cm/h) and high permeability (greater than 5 cm/h). The soils data also provided guidance in the initial selection and subsequent modification (during calibration) of soil related parameters that affect infiltration capacity, upper and lower zone storages, interflow and recession rate, and groundwater recession rate.

The SMR model used several parameters from the soil databases for each soil layer, including depth, bulk density, and saturated conductivity (K_s) (referred to as permeability in the soil surveys, US Department of Agriculture (USDA), 1993). Average values were used for soil parameters that were reported as a range in the databases. The primary texture class listed in the soils database for each soil layer was used to determine water retention properties, as presented in Maidment (1993).

Parameter values for aquifer recharge were calculated for use in SMR from an analysis of recession hydrographs. First, soils were assigned to one of two drainage classes through a detailed consideration of the soil descriptions in the soil surveys (Table 1). Soils with poor drainage were assigned a percolation rate of 0.1 mm/day (Boll et al., 1998), and freely draining soils were assigned a percolation rate of 1.5 mm/day, which was based on an analysis of low flows during low ET and non-winter months, when baseflow was assumed to reflect the subsurface percolation rate. Aquifer recharge from the soil profile was applied only if micropore storage was satisfied for the given time step.

2.5. Land use/land cover data

The land use/land cover map was developed by converting the 30 m Multi-Resolution Land Characteristics (MRLC) land use/land cover map to a 10 m grid size and merging this map with 10 m grid size digital maps of roads and wetlands (delineated in the National Wetlands Inventory, US Fish and Wildlife Service, 2000).

The HSPF model used the land use/land cover as the third attribute for HRU definition. These data were grouped into seven classes: low density residential, commercial (including roads and commercial, industrial, and high-density residential land uses), forest, agricultural, wetlands and ponds, open grass, and urban recreational grass. Low density residential and commercial land use/land cover classes were divided into effective impervious areas, which conceptually represent areas hydrologically connected to the local surface-drainage network, and disturbed areas, which include the remaining grass, forested, and ineffective impervious areas.

The SMR model used land use/land cover data only to estimate evapotranspiration. This entailed assigning a vegetation coefficient to each land use/land cover class for each month as described by Allen (1998).

2.6. Meteorological data

Meteorological data for HSPF included hourly precipitation as recorded at the National Weather Service (NWS) observation station in Victor, NY (located 0.25 km east of the study area). Hourly recorded air and dew point temperatures, wind speed, cloud cover, and computed time series of potential evapotranspiration and solar radiation were obtained from the NWS station at the Greater Rochester International Airport (located 12 km northeast of the study area).

Meteorological data for SMR included daily precipitation recorded at both the Victor and Rochester NWS stations (applied as distributed input through an inverse-distance weighting factor), and the daily average temperature recorded at Rochester (applied as distributed input through an adiabatic lapse rate), which adjusted the temperature data for differences in elevation between the grid cell and the weather station to account for spatial variability in snowmelt. HSPF can adjust temperature for the average elevation difference between the weather station and each HRU from an adiabatic lapse rate, but this option only affects the results in mountainous areas.

2.7. Model-specific details of application to study area

2.7.1. HSPF application

HRUs were defined as unique combinations of land use/land cover, slope, and soil permeability (e.g. forest cover, low slope, high permeability). Each

10 m^2 area in the watershed was characterized by a given HRU, and the area encompassed by each HRU within each subbasin of the study area was calculated. These areas were assumed to possess similar hydrologic characteristics and to respond in a similar manner to meteorological inputs.

Next, relations among stage, storage, and discharge were developed for the main stream channel in each subbasin from field measurements of channel geometry and GIS analysis of reach length and slope. The relation between the effective impervious area (EIA) and housing density was estimated from a GIS analysis of land use/land cover and tax parcel data.

Initial parameter values were selected on the basis of field data, soil survey data, and GIS analysis wherever possible. Parameters not directly measured were estimated from information given in HSPF reference materials, including BASINS Technical Note 6 (US Environmental Protection Agency (USEPA), 2000) and previously developed models that simulated watersheds with similar soil types, land uses, climatic zones, and drainage basin sizes as described in published reports or available in HSPFParm, an interactive database of HSPF model parameters (Donigian et al., 1999). Runoff processes were simulated at an hourly time step. Parameter values for each HRU were adjusted independently during calibration over the seven-year simulation period through HSPEXP, a computer program developed to assist modelers in the calibration of HSPF (Lumb et al., 1994).

2.7.2. SMR application

SMR parameter values were obtained from available soil databases or calculated from streamflow analyses. The watershed area (102 km^2) and the optimal grid cell size for representing hydrologic processes (10 m) produced a grid of roughly 1 million grid cells. Simulation time per year of the simulation period was about 8 h on a computer with a 1.4 GHz processor, which precluded true calibration of the model in the form of parameter optimization. The 'calibration' stage was completed when it appeared that the input data were error free and the output data agreed closely with field-measured values.

Sparsity of aquifer data required a semi-distributed approach, patterned from that of TOPMODEL (Beven et al., 1995), to simulate baseflow contribution to streamflow. Streamflow analysis determined the baseflow parameters used in Eq. (2) to be as follows: Q_o (the lowest recorded streamflow in the period of record) was 0.18 mm/day, and m, which was based on an analysis of 12 recession curves at the US Geological Survey (USGS) streamflow monitoring site at the downstream end of the study area, ranged from 4.8 to 8.1 mm, with an arithmetic and geometric mean of 6.3 mm. Analysis of precipitation and streamflow records indicated that streamflow was generated in response to rainstorms of 1 mm or greater. The parameter t (time since precipitation) was reset for any precipitation greater than or equal to 1 mm.

2.8. Method of evaluation and comparison of results

The SMR and HSPF models' results were evaluated on a daily time step basis for the simulation period (July 1991–September 1998). This seven-year period ensured that the calibration encompassed the full ranges for hydrologic conditions and flow regimes (e.g. several high flows, wet and dry years, and wet and dry periods). Hourly HSPF results were aggregated to a daily time step prior to the comparison. Model evaluation involved comparison of the simulated streamflow of Irondequoit Creek at Railroad Mills with the measured streamflow. A series of seven winter (November–April) and seven summer (May–October) periods within the simulation period permitted a detailed analysis of model performance over time and under a variety of hydrologic conditions as well as a direct comparison between the performances of the two models.

2.8.1. Evaluation

The HSPF model received no evaluation other than the comparison of simulated and measured flow because of the conceptual nature of its parameters; many of the storages used by HSPF are not defined explicitly and cannot be directly measured (Jacomino and Fields, 1997). Further, streamflow gives an integral response that is possible to accurately simulate with several combinations of parameter values (Beven and Freer, 2001). Finally, comparison of individual parameters with field measurements was impossible because the parameter values for each

HRU represented an average or lumped value for the area represented by the HRU.

The SMR model permitted and allowed further validation beyond the integral streamflow response by comparison of the measured and simulated distributed results. For this purpose, an undulating, grassy hillslope in the study area, which had exhibited saturated conditions, even during dry periods, was selected for spatially distributed data collection. Soil moisture was measured through time-domain reflectometry (TDR) at sampling stations 10 m intervals apart along five 160 m long parallel transects, established 10 m apart and perpendicular to the predominant slope of the hill. At each sampling location, three TDR measurements were taken at 30 cm increments across the slope for the 0–12 cm soil horizon and were compared with SMR results for the same location. The Global Positioning System (GPS) was used to identify the latitude–longitude coordinates of the TDR measurement sites. Comparison between field measurements and model output was made through normalized indices of each data set. A field saturation index (FSI) was developed for use in SMR evaluation. The average of three TDR measurements taken at each sample location (θ_{TDRavg}) was normalized by the average TDR reading for saturated soil at the hillslope (θ_{TDRsat}) ($n = 15$), yielding the FSI equation scaled from 0 to 100:

$$\mathrm{FSI} = 100^{*}\left(\frac{\theta_{\mathrm{TDRavg}}}{\theta_{\mathrm{TDRsat}}}\right) \tag{3}$$

Similarly, a model saturation index (MSL), also scaled 0–100, was calculated by normalizing the soil moisture content of each grid cell by the saturated moisture content of the grid cell, where 100 represented a fully saturated cell. The soil moisture content was calculated at each time step, and the saturated moisture content was a parameter derived from soil survey data as described previously. The computed indices allowed comparison between model predictions and a readily measurable property for the hillslope.

2.8.2. Comparison

Early model comparison studies used graphical and statistical methods to evaluate results (World Meteorological Organization, 1975). Evaluation of graphical criteria is subjective, however, as discussed by Houghton-Carr (1999), and no 'best' statistical-quality criterion has been identified for hydrologic models (Weglarczyk, 1998). Therefore, three objective-function assessment criteria were used to compare HSPF and SMR model output; this was done in accordance with a method described by Perrin et al. (2001). The criteria were the Nash–Sutcliffe model efficiency, (E_{f}) (Nash and Sutcliffe, 1970), the mean absolute error (MAE), and the mean cumulative error (MCE). E_{f}, which ranges from $-\infty$ to 1, where 1 represents a perfect fit, is given as:

$$E_{\mathrm{f}} = 1 - \frac{\sum_{i=1}^{n}(Q_{\mathrm{obs},i} - Q_{\mathrm{sim},i})^2}{\sum_{i=1}^{n}(Q_{\mathrm{obs},i} - \overline{Q_{\mathrm{obs},i}})^2} \tag{4}$$

where $Q_{\mathrm{obs},i}$ = observed streamflow at time step i, $\overline{Q_{\mathrm{obs},i}}$ = mean observed streamflow during the evaluation period, and $Q_{\mathrm{sim},i}$ = model simulated streamflow at time step i. $\overline{Q_{\mathrm{obs},i}}$ was calculated for each of the comparison periods and used in the calculation of E_{f}, in accordance with suggestions made in Martinec and Rango (1989).

The second criterion, also transformed to a scale of $-\infty$ to 1, was derived from the mean absolute model error, and applied as the MAE:

$$\mathrm{MAE} = 1 - \frac{\sum_{i=1}^{n}|Q_{\mathrm{obs},i} - Q_{\mathrm{sim},i}|}{\sum_{i=1}^{n}|Q_{\mathrm{obs},i} - \overline{Q_{\mathrm{obs},i}}|} \tag{5}$$

The third criterion was derived from the MCE, and likewise was transformed to a scale of $-\infty$ to 1. MCE, which yields an assessment of the streamflow volume predicted over the simulated period, is given as:

$$\mathrm{MCE} = 1 - \left|\sqrt{\frac{\sum_{i=1}^{n} Q_{\mathrm{sim},i}}{\sum_{i=1}^{n} Q_{\mathrm{obs},i}}} - \sqrt{\frac{\sum_{i=1}^{n} Q_{\mathrm{obs},i}}{\sum_{i=1}^{n} Q_{\mathrm{sim},i}}}\right| \tag{6}$$

The numerical evaluation criteria were applied to the model-simulated streamflow for the entire study period, as well as for the summer and winter periods (Table 2). The three evaluation criteria for the summer and winter periods were based solely on the streamflow data for the summer or winter period of concern. For example, only the observed streamflow data for the 1992 summer period were used to calculate the three evaluation criteria for the 1992 summer. For the purposes of model evaluation as presented in this paper, a dry summer (or winter) period was one where

Table 2
Summary of HSPF and SMR model results for simulations of sreamflow in the Irondequoit Creek at Railroad Mills for entire simulation period (July 1, 1991–Sept. 30, 1998) and for winter and summer seasons of that period

Period[a]	Mean streamflow (mm/day)	E_f [b]		MAE[c]		MCE[d]	
		HSPF	SMR	HSPF	SMR	HSPF	SMR
Entire simulation period (July 1, 1991 – Sept. 30, 1998)	1.0	0.67	0.65	0.46	0.50	0.96	0.97
Winter 1991–1992 (dry)	0.9	0.78	0.64	0.52	0.40	0.95	0.89
Summer 1992	1.0	0.35	0.72	0.22	0.53	0.76	0.91
Winter 1992–1993	2.0	0.60	0.51	0.40	0.49	0.90	0.86
Summer 1993	0.5	0.29	0.24	0.07	0.05	0.65	0.72
Winter 1993–1994	1.2	0.62	0.60	0.50	0.50	0.96	0.94
Summer 1994	0.6	0.72	0.38	0.43	0.13	0.88	0.70
Winter 1994–1995	0.9	0.39	0.59	0.16	0.32	0.78	0.98
Summer 1995	0.3	0.67	0.40	−0.12	0.29	0.62	0.94
Winter 1995–1996	1.2	0.58	0.56	0.38	0.36	0.96	0.99
Summer 1996 (wet)	1.0	0.69	0.76	0.47	0.50	0.82	0.95
Winter 1996–1997	1.4	0.63	0.67	0.37	0.37	0.97	0.98
Summer 1997 (dry)	0.6	0.53	0.55	0.43	0.43	0.90	0.95
Winter 1997–1998 (wet)	1.6	0.86	0.61	0.38	0.42	0.88	0.99
Summer 1998	0.7	−1.38	0.19	−0.16	0.05	0.64	0.71
Summer mean	0.7	0.27	0.46	0.19	0.28	0.75	0.84
Winter mean	1.3	0.64	0.60	0.39	0.41	0.91	0.95

[a] Nash–Sutcliffe model efficiency.
[b] Winter = November–April. Summer = May–October.
[c] Mean absolute error.
[d] Mean cumulative error.

the mean streamflow was less than the seven-year (1991–1998) average summer (or winter) streamflow, and a wet summer (or winter) period was one where the mean streamflow was greater than the seven-year average summer (or winter) streamflow.

3. Results and discussion

The hydrographs in Figs. 4 and 5, which show high flow peaks during periods of extended rainfall and rapidly decreasing flows shortly after the rainfall stops, are characteristic of the region. Both HSPF and SMR simulated streamflows were compared with measured streamflow and with each other. Distributed soil moisture content predicted by SMR is compared with field-measured soil moisture content.

3.1. HSPF results

The simulated HSPF streamflow for Irondequoit Creek at Railroad Mills for the seven-year simulation period is plotted with the measured values in Fig. 4. The two hydrographs show acceptable agreement, although an apparent tendency towards underprediction is evident during the summer periods. Simulated peak flows are reasonably consistent with measured peaks, especially during snowmelt related high flows.

The three evaluation criteria for HSPF for the simulation period indicated that overall model performance was satisfactory (Table 2). The E_f value for the entire period is 0.67, and the MCE value is 0.96. The MAE for the entire period is 0.46.

3.2. Integrated SMR results

The simulated SMR streamflow for Irondequoit Creek at Railroad Mills is plotted with the measured values in Fig. 5. Despite the limited calibration of SMR, the two hydrographs show acceptable agreement, although the simulated summer flows appear to be more accurate than the simulated winter flows.

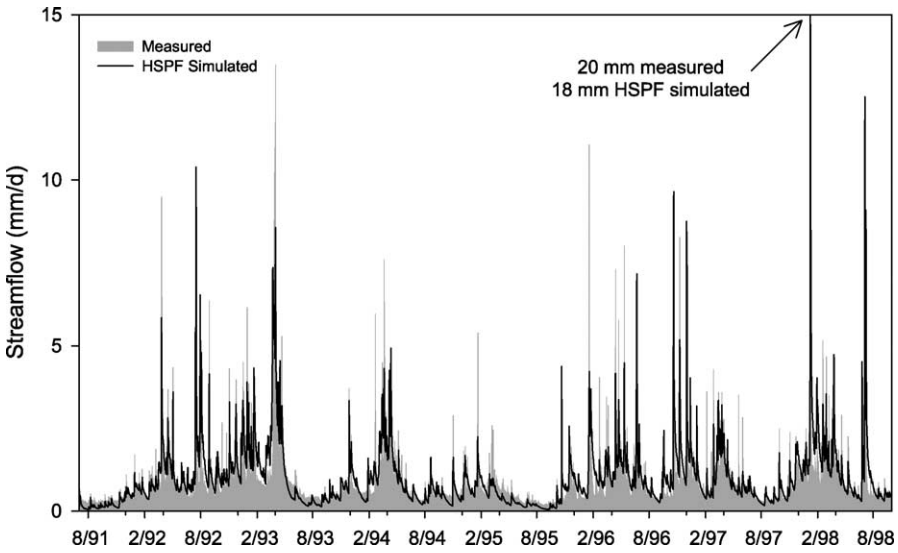

Fig. 4. Measured and HSPF simulated streamflow of Irondequoit Creek at Railroad Mills during the seven-year simulation period.

During the summer low flow periods, however, SMR simulated flows show small peaks on some rainfall days whereas the observed streamflow records do not. This discrepancy results because in SMR all saturation excess runoff is directly routed to the stream, whereas, in reality, this runoff is likely to infiltrate either before or after it reaches the stream. Despite this source of error, the overall evaluation criteria were reasonable. The E_f value for 1991–1998 is 0.65, the MCE value is 0.97, and the MAE value is 0.50.

3.3. Comparison of models

Comparison of the HSPF hydrograph with the integrated SMR hydrograph (Fig. 6) clearly shows

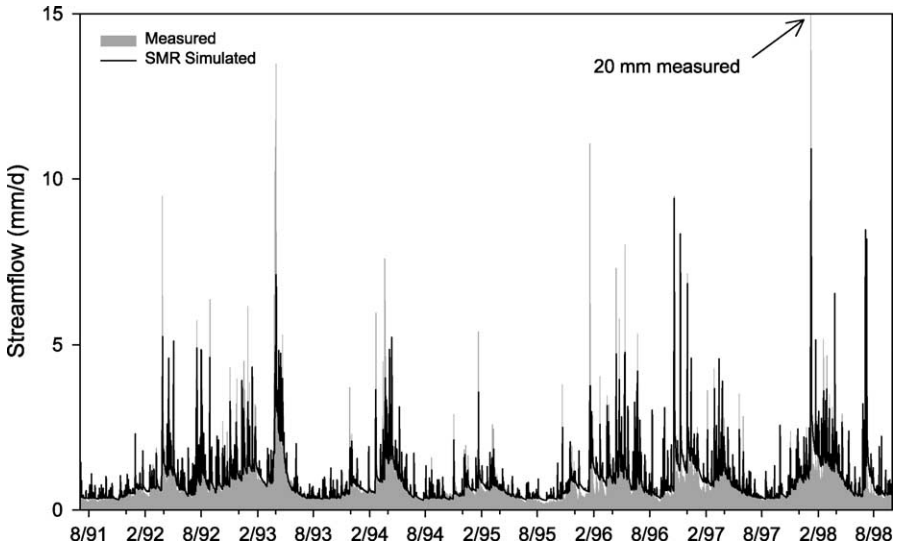

Fig. 5. Measured and SMR simulated streamflow of Irondequoit Creek at Railroad Mills during the seven-year simulation period.

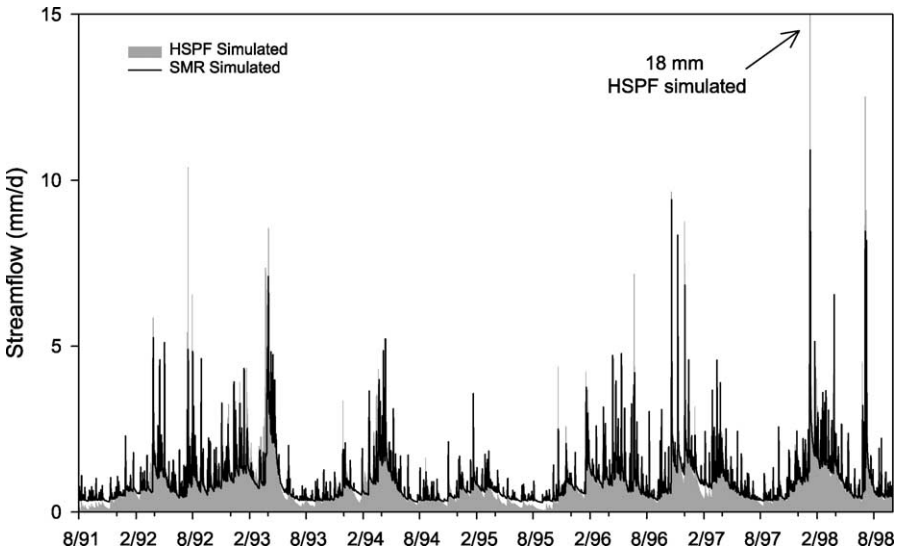

Fig. 6. HSPF and SMR simulated streamflow of Irondequoit Creek at Railroad Mills during the seven-year simulation period.

minimal differences throughout the seven-year simulation period, despite the different runoff mechanisms used by HSPF and SMR. Both models used the same precipitation as input and calculated similar evaporation amounts. Streamflow, as the integrated response of the watershed, should equal the balance of precipitation and evaporation over a sufficiently long time and, therefore, would be independent of the runoff mechanism. This fact is especially true for a watershed that is dominated by relatively shallow soils over a hardpan and, consequently, low soil water storage, for which SMR was specifically developed. Despite the overall agreement in streamflow simulations, small differences exist. For example, in the summer periods SMR gave more accurate results than HSPF as indicated by the E_f values in Table 2. E_f values for SMR were greater than those for HSPF for four of the seven summer periods, and the mean summer E_f values were 0.46 for SMR and 0.27 for HSPF. However, these summary statistics are greatly influenced by the atypically low values computed for the summer of 1998. If these 1998 values, which are based on the period May–September rather than May–October, are ignored, then comparable E_f values for SMR (0.51) and HSPF (0.54) result. For the winter periods, HSPF results were slightly more accurate than SMR; E_f values for HSPF were greater than those for SMR for five of the seven winter periods and the mean winter E_f values were 0.64 for HSPF and 0.60 for SMR. The two models' accuracy for winter periods was comparable (MAE of 0.39 for HSPF and 0.41 for SMR; and MCE of 0.91 for HSPF and 0.95 for SMR, but the SMR evaluation criteria values for the summer periods were greater than those of HSPF (MAE of 0.19 for HSPF and 0.28 for SMR, and MCE of 0.75 for HSPF and 0.84 for SMR). The greatest errors for both models were in the dry summer simulations.

3.3.1. Simulated winter periods

The measured and simulated streamflows for the wet winter period (1997–1998) are plotted in Fig. 7 with the dry winter period (1991–1992) plotted in Fig. 7B. These plots indicate that HSPF predicted winter peaks well, especially the snowmelt-generated high flow of January 1998, which was the greatest measured streamflow during the period of record. HSPF overpredicted some of the winter low flows, however. These observations are confirmed by the evaluation criteria in Table 2. The good fit for HSPF during the winter periods was evidenced by the mean E_f value of 0.64 for the seven winter periods. The HSPF error, as expressed by the MAE and MCE

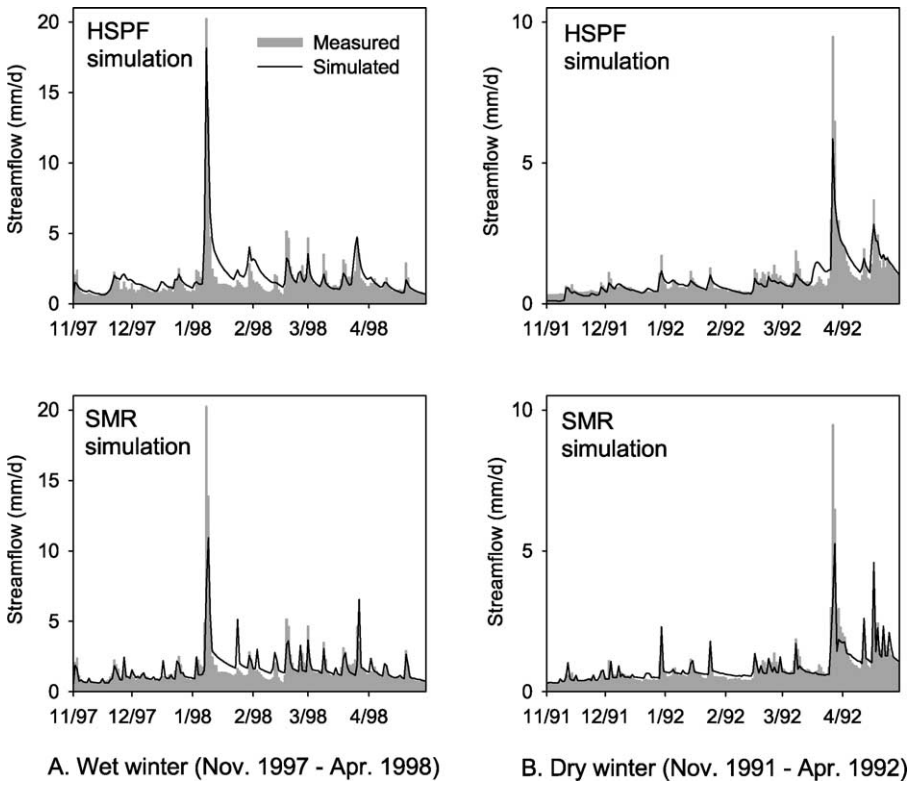

Fig. 7. Measured and simulated (HSPF and SMR) streamflow of Irondequoit Creek at Railroad Mills during representative wet and dry winters. A. Wet winter (November 1997–April 1998). B. Dry winter (November 1991–April 1992).

values (Table 2), was low; the mean MCE value for the seven winters, 0.91, indicates an acceptable simulation of total streamflow volume during the winters. The average MAE value for the seven winters, 0.39, is acceptable in that MAE is influenced by many factors that affect the performance of watershed models, especially the difficulty of representing watershed-scale processes from point data. The highest MAE value for any period by either model was 0.53.

SMR results for the two winters (Fig. 7A and B) show large discrepancies between measured and simulated streamflow during high flow periods generated by snowmelt; these discrepancies are likely related to the simplified temperature-index method that SMR uses to calculate snowmelt. Nevertheless, the three evaluation criteria (Table 2) indicate that SMR simulated the seven winter periods well, with a mean E_f of 0.60, MAE of 0.41, and MCE of 0.95. The simulation results for the winter periods confirm that since the streamflow at the outlet is averaged over the whole watershed, differences in snowmelt input in the water balance are much more significant than runoff mechanisms for determining the temporal streamflow characteristics.

3.3.2. Simulated summer periods

The measured and simulated streamflows for a wet summer (1996) and a dry summer (1997) are plotted in Fig. 8. HSPF simulated peak flows of the wet summer well (Fig. 8A), but often underpredicted low flows during the dry summer (Fig. 8B). Summer E_f values for HSPF ranged from 0.72 to 1.38, with a mean value of 0.27. The HSPF mean MAE value for the seven summer periods for HSPF is 0.19—considerably lower than that for winter periods (0.39).

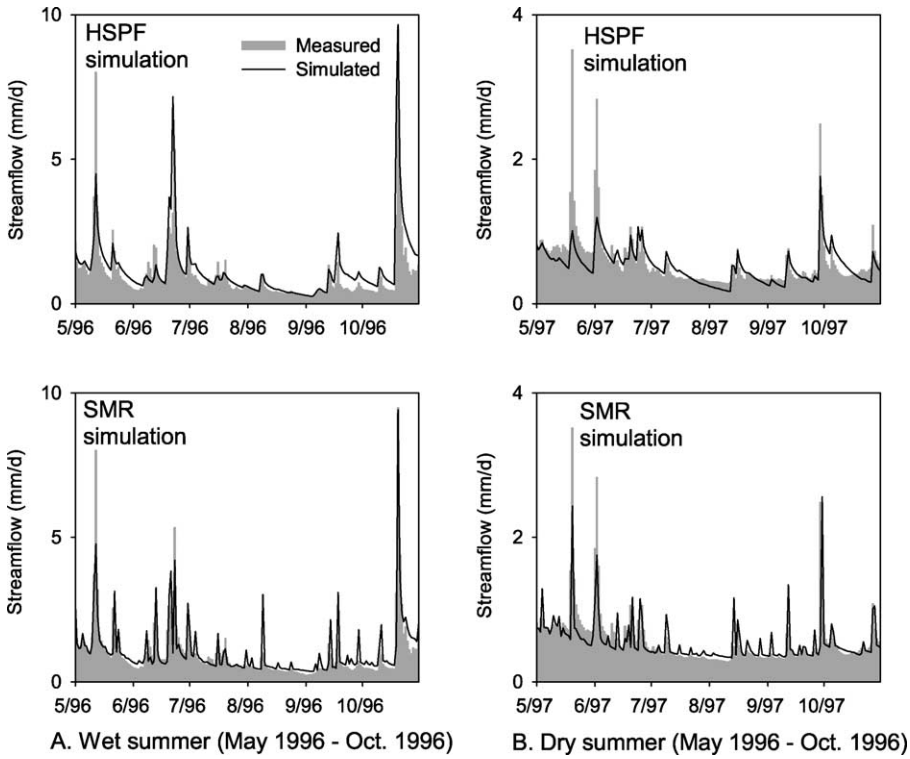

Fig. 8. Measured and simulated (HSPF and SMR) streamflow of Irondequoit Creek at Railroad Mills during representative wet and dry summers. A. Wet summer (May–October 1996). B. Dry summer (May–October 1997).

The summer SMR plots in Fig. 8A and B show that SMR predicted wet and dry summer streamflows well; the SMR E_f value for the wet summer was 0.76, and that for the dry summer was 0.55. The best summer SMR results, as indicated by the three evaluation criteria, correspond to wet summers, during which saturation-excess runoff contributed a greater percentage of streamflow than during dry summers.

3.4. Distributed SMR results

The distributed SMR model results (soil moisture content) were compared with field measurements and are presented in terms of model and field saturation indices (MSI and FSI). Unlike streamflow, validating a model with its distributed output is a much better test for proving the validity of the runoff mechanism. However, a comparison between spatially distributed field data and HSPF results was not possible, as previously indicated. The SMR model accurately predicted soil moisture distribution on the hillslope along transect A during dry and wet periods (Fig. 9). This was demonstrated by r^2 values in the range of 0.7–0.8, and E_f values in the range of 0.64–0.80. The locations of soil moisture peaks in the field and those predicted by the model indices (corresponding to topographic convergence of subsurface flow pathways) frequently disagreed by one or two grid cells; however, this indicates that the 10 m scale DEM may have been insufficiently fine to capture small changes in surface slope within the watershed. In GIS analysis, the slope for each grid cell was calculated from the differences in elevation of the surrounding grid cells. Each grid cell was assigned an average elevation for the 10 m by 10 m land surface area it represented. This averaging of elevations may account for the differences between field and simulated values, in that the slope is a key

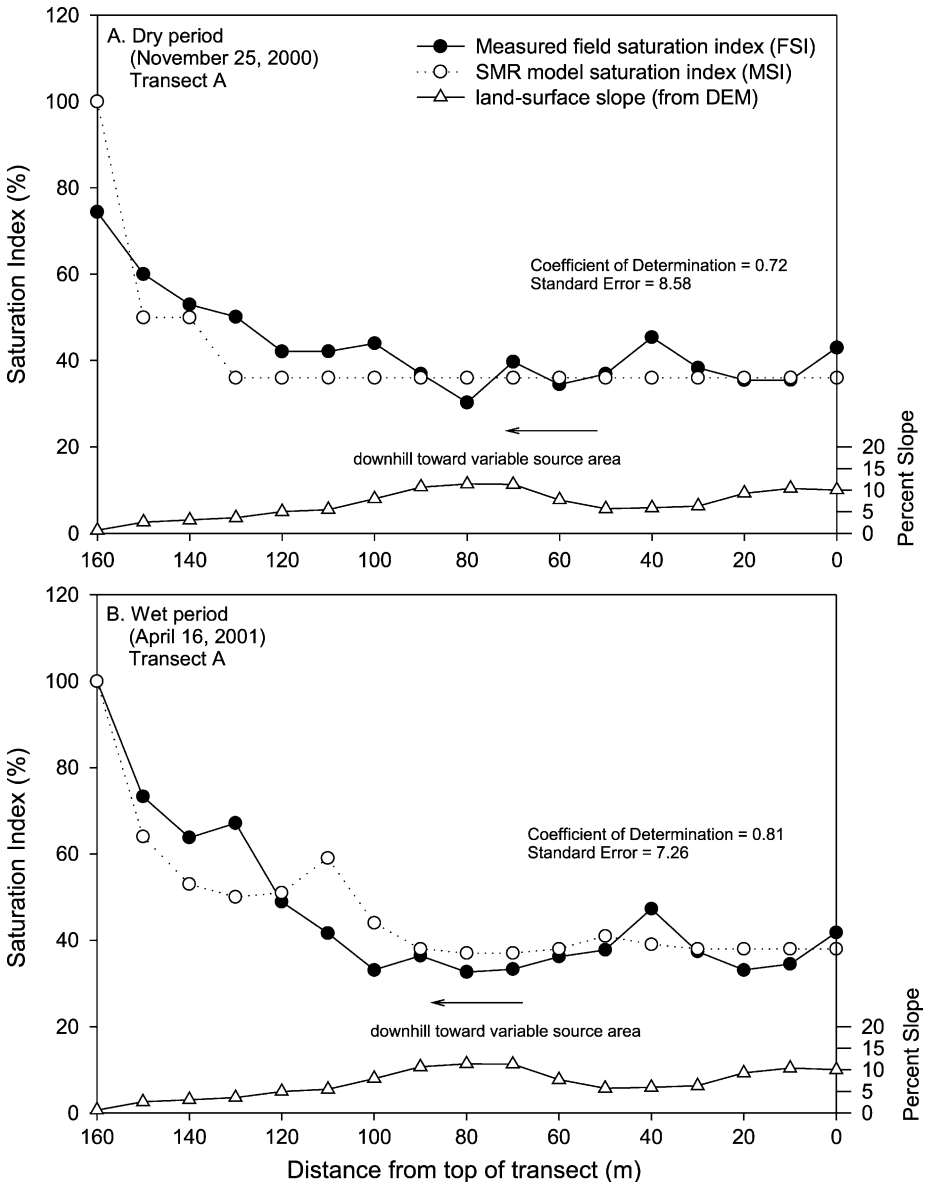

Fig. 9. Field and SMR simulated soil-saturation indices in the Irondequoit Creek basin. A. Representative dry period (November 2000) along transect A. B. Representative wet period (April 2001) along transect A.

factor in lateral subsurface flow in SMR (see Eq. (1)). In addition, flat slopes are problematic for SMR because the model routes lateral flow between a grid cell and its neighboring cells according to elevation differences. Differences in water table elevation on slopes of less than 2% become increasingly important in determining lateral flow, as well as overland seepage, from one cell to the next. The plot of percent saturation index as a function of distance from the top of transect B (Fig. 10) indicates that the field and model saturation indices were in agreement until

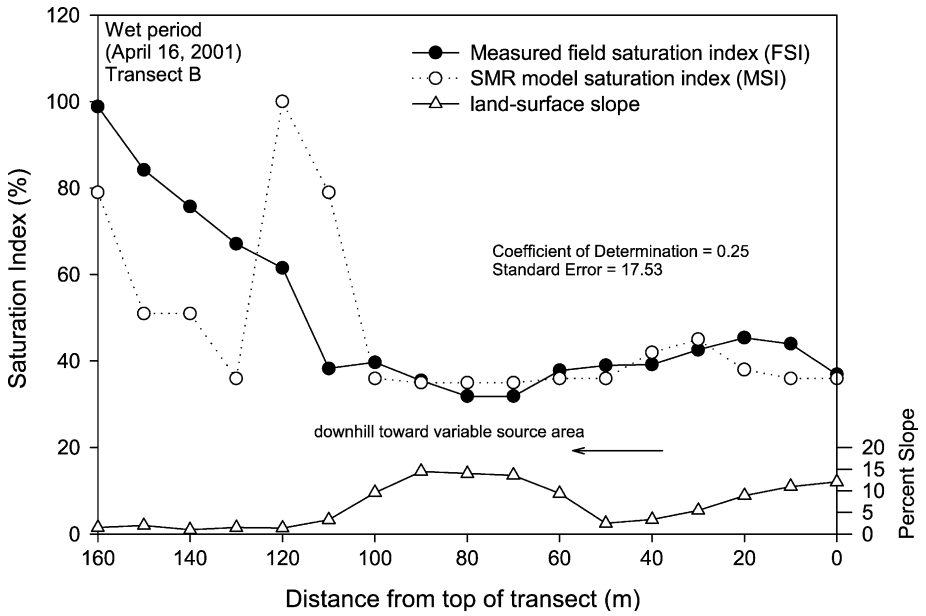

Fig. 10. Field and SMR simulated soil-saturation indices in the Irondequoit Creek basin: Representative wet period (April 2001) along transect B.

the slope dropped below 2%, at which point the indices diverged. The general trend was well predicted, however.

4. Conclusions

HSPF and SMR, two watershed models that differ in structure and representation of hydrologic processes, including runoff generation, snowmelt, and baseflow, were evaluated for their ability to simulate streamflow (and, in the case of SMR, to identify areas of saturation in the watershed) over a seven-year period in the upper part of the Irondequoit Creek watershed in Monroe County, NY. Both models gave adequate simulations of streamflow. Statistical evaluation criteria that were applied to the available period-of-record data showed both models to produce acceptable results for the entire period. However, a detailed seasonal evaluation of the seven summer and winter periods revealed seasonal differences in accuracy.

The comparative analysis indicated that despite the dissimilarity in runoff mechanisms, there was close agreement in the overall simulation results. Nevertheless, small differences existed: (1) SMR was more accurate than HSPF in the simulation of streamflow during the summer periods, when saturation excess is a major factor in runoff generation, and (2) HSPF simulated streamflow more accurately than SMR during the winter snowmelt periods. The timing of simulated peaks in streamflow was directly related to the accuracy of snowmelt prediction. HSPF incorporates rigorous energy-balance equations, whereas the current version of SMR uses a simple water balance method. Furthermore, infiltration excess, as modeled by HSPF, may occur in some parts of the watershed during winter when the ground is frozen. Also, snowmelt or rainfall leaves the soil either as runoff or as interflow and is not strongly related to the infiltration capacity of the soil.

The results of this study also demonstrated that the hydrologic processes in a watershed, and the purpose of the modeling effort (integral streamflow response or distributed output, such as identification of runoff producing area or estimation of soil moisture content) need to be defined before a hydrologic model intended to simulate these processes is selected. The runoff-generating mechanism used by a model might be

inconsequential over a long simulation period, but can affect simulation accuracy on a seasonal basis. Although either model could be used to predict streamflow, the semi-distributed conceptual nature of HSPF precludes its use for predicting spatial distribution of soil moisture content or other physically measurable parameters at specific locations within the watershed. SMR was shown to be useful for analysis of spatially distributed processes.

References

Allen, R.G., 1998. Crop Evapotranspiration—Guidelines for Computing Crop Water Requirements, FAO, Rome.

Berris, S.N., 1995. Conceptualization and Simulation of Runoff Generation from Rainfall for Three Basins in Thurston County, Washington. USGS Water-Resources Investigations Report 94-4038, 149 p.

Beven, K., Freer, J., 2001. Equifinality, data assimilation, and uncertainty estimation in mechanistic modelling of complex environmental systems using the GLUE methodology. J. Hydrol. 249, 11–29.

Beven, K., Lamb, R., Quinn, P., Romanowicz, R., Freer, J., 1995. TOPMODEL. In: Singh, V.P., (Ed.), Computer Models of Watershed Hydrology, Water Resources Pubs, Highlands Ranch, CO, pp. 627–668.

Bicknell, B.R., Imhoff, J.C., Kittle, J.L. Jr., Donigian, A.S., Johanson, R.C., 1997. Hydrological Simulation Program—FORTRAN. User's Manual for Release 11. EPA-600/R-97-080, USEPA, Athens, GA, 755 p.

Boll, J., Brooks, E.S., Campbell, C.R., Stockle, C.O., Young, S.K., Hammel, J.E., McDaniel, P.A., 1998. Progress Toward Development of a GIS-based Water Quality Management Tool for Small Rural Watersheds: Modification and Application of a Distributed Model. Paper No. 982230, American Society of Agricultural Engineers, St. Joseph, MI.

Crawford, H.H., Linsley, R.K., 1966. Digital Simulation in Hydrology: Stanford Watershed Model IV. Technical Report No. 39, Dept. of Civil Eng., Stanford University, Stanford, CA.

DeGaetano, A.T., Eggleston, K.L., Knapp, W.W., 1994. Daily Evapotranspiration and Soil Moisture Estimates for the Northeastern US. Research Series No. RR94-1, Northeast Regional Climate Center, Cornell University, Ithaca, NY.

Donigian, A.S. Jr., Crawford, N.H., 1976. Modeling Nonpoint Pollution from the Land Surface. EPA-600/3-76-083, USEPA, Athens, GA, 166 p.

Donigian, A.S. Jr., Davis, H.H., 1978. User's Manual for Agricultural Runoff Management (ARM) Model. EPA-600/3-78-080, USEPA, Athens, GA, 112 p.

Donigian, A.S., Jr., Huber, W.C., 1991. Modeling of Nonpoint Source Water Quality in Urban and Non-Urban Areas. EPA-600/3-91-039, USEPA, Athens, GA, 78 p.

Donigian, A.S. Jr., Bicknell, B.R., Imhoff, J.C., 1995. Hydrological simulation program—FORTRAN (HSPF). In: Singh, V.P., (Ed.), Computer Models of Watershed Hydrology, Water Resources Pubs, Highlands Ranch, CO, pp. 395–442.

Donigian, A.S. Jr., Chinnaswamy, R.V., Jobes, T.H., 1997. Conceptual Design of Multipurpose Detention Facilities for Flood Protection and Nonpoint Source Pollution Control, Aqua Terra Consultants, Mountain View, CA, 151 p.

Donigian, A.S. Jr., Imhoff, J.C., Kittle, J.L., 1999. HSPFParm—An Interactive Database of HSPF Model Parameters, Version 1.0. EPA-823-R-99-004, USEPA, Washington, DC, 40 p.

Dunne, T., 1978. Field studies of hillslope processes. In: Kirkby, M.J., (Ed.), Hillslope Hydrology, Wiley, Chichester, UK, pp. 227–294.

EarthInfo, Inc., 1993. SCS Soils-5. Boulder, CO.

Fontaine, T.A., Jacomino, V.M.F., 1997. Sensitivity analysis of simulated contaminated sediment transport. J. Am. Water Resour. Assoc. 33, 313–326.

Franchini, M., Pacciani, M., 1991. Comparative-analysis of several conceptual rainfall runoff models. J. Hydrol. 122, 161–219.

Frankenberger, J.R., Brooks, E.S., Walter, M.T., Walter, M.F., Steenhuis, T.S., 1999. A GIS-based variable source area hydrology model. Hydrol. Proc. 13, 805–822.

Gan, T.Y., Dlamini, E.M., Biftu, G.F., 1997. Effects of model complexity and structure, data quality, and objective functions on hydrologic modeling. J. Hydrol. 192, 81–103.

Heffner, R.L., Goodman, S.D., 1973. Soil Survey of Monroe County, New York, USDA-Soil Conservation Service, Washington, DC, 172 p.

Hornlein, J.F., Szabo, C.O., Zajd Jr., H.J., Mulks, R.L., 1999. Water Resources Data, New York, Water Year 1999, Vol. 3, Western New York. USGS Water-Data Report NY-99-3, 349 p.

Houghton-Carr, H.A., 1999. Assessment criteria for simple conceptual daily rainfall-runoff models. Hydrol. Sci. J. 44, 2637–2649.

Hydrocomp, Inc., 1977. Hydrocomp Water Quality Operations Manual, Hydrocomp, Inc, Palo Alto, CA.

Jacomino, V.M.F., Fields, D.E., 1997. A critical approach to the calibration of a watershed model. J. Am. Water Resour. Assoc. 33, 143–154.

Jarvis, N., Larsson, M., 2001. Modeling macropore flow in soils: field validation and use for management purposes. In: Conceptual Models of Flow and Transport in the Fractured Vadose Zone, National Research Council, Panel on Conceptual Models of Flow and Transport in the Fractured Vadose Zone, National Academy Press, Washington, DC, pp. 189–216.

Kappel, W.M., Young, R.A., 1989. Glacial History and Geohydrology of the Irondequoit Creek Valley, Monroe County, New York. USGS Water-Resources Investigations Report 88-4145, 34 p.

Kuo, W.L., Steenhuis, T.S., McCulloch, C.E., Mohler, C.L., Weinstein, D.A., DeGloria, S.D., Swaney, D.P., 1999. Effect of grid size on runoff and soil moisture for a variable source area hydrology model. Water Resour. Res. 35, 3419–3428.

Lahlou, M., Shoemaker, L., Choundhury, S., Elmer, R., Hu, A., Manguerra, H., Parker, A., 1998. Better Assessment Science

Integrating Point and Nonpoint Sources—BASINS. EPA-823-B-98-006, USEPA, Washington, DC.

Laroche, A.M., Gallichand, J., Lagace, R., Pesant, A., 1996. Simulating atrazine transport with HSPF in an agricultural watershed. ASCE J. Environ. Engng. 122, 622–630.

Lumb, A.M., McCammon, R.B., Kittle, J.L., Jr., 1994. User's Manual for the Expert System (HSPEXP) for Calibration of the Hydrological Simulation Program-Fortran. USGS Water-Resources Investigations Report 94-4168, 102 p.

Maidment, D.R., 1993. Handbook of Hydrology, McGraw-Hill, New York.

Martinec, J., Rango, A., 1989. Merits of statistical criteria for the performance of hydrological models. Water Resour. Bull. 25, 421–432.

Michaud, J., Sorooshian, S., 1994. Comparison of simple versus complex distributed runoff models on a midsized semiarid watershed. Water Resour. Res. 30, 593–605.

Nash, J.E., Sutcliffe, J.V., 1970. River flow forecasting through conceptual models, Part I—a discussion of principles. J. Hydrol. 10, 238–250.

Pearson, C.S., Cline, M.G., 1958. Soil Survey of Ontario and Yates Counties, New York, USDA-Soil Conservation Service, Washington, DC, 126 p..

Perrin, C., Michel, C., Andreassian, V., 2001. Does a large number of parameters enhance model performance? Comparative assessment of common catchment model structures on 429 catchments. J. Hydrol. 242, 275–301.

Refsgaard, J.C., Knudsen, J., 1996. Operational validation and intercomparison of different types of hydrological models. Water Resour. Res. 32, 2189–2202.

Srinivasan, M.S., Hamlett, J.M., Day, R.L., Sams, J.I., Peterson, G.W., 1998. Hydrologic modeling of two glaciated watersheds in northeast Pennsylvania. J. Am. Water Resour. Assoc. 34, 963–978.

Thornthwaite, C.W., Mather, J.R., 1955. The Water Balance. Pub. No. 8, Laboratory of Climatology, Centerton, NJ.

US Army Corps of Engineers, 1960. Engineering and Design: Runoff from Snowmelt. EM 1110-2-1406, US Army Corps of Engineers, Washington, DC.

US Department of Agriculture (USDA), 1993. Soil Survey Manual. Revised Edition, USDA-Natural Resources Conservation Service, Soil Survey Division, Washington, DC.

US Environmental Protection Agency (USEPA), 2000. BASINS Technical Note 6—Estimating Hydrology and Hydraulic Parameters for HSPF. EPA-823-R-00-012, USEPA, Washington, DC, 24 p.

US Fish and Wildlife Service, 2000. Digital Map of National Wetlands Inventory, 2000. Accessed March 9, 2000 at URL www.nwi.fws.gov/maps.

Walter, M.T., Walter, M.F., Brooks, E.S., Steenhuis, T.S., Boll, J., Weiler, K., 2000. Hydrologically sensitive areas: variable source area hydrology implications for water quality risk assessment. J. Soil Water Conserv. 55, 277–284.

Weglarczyk, S., 1998. The interdependence and applicability of some statistical quality measures for hydrological models. J. Hydrol. 206, 98–103.

World Meteorological Organization (WMO), 1975. Intercomparison of Conceptual Models used in Operational Hydrological Forecasting. Operational Hydrology Report 7, WMO, Geneva.

World Meteorological Organization (WMO), 1986. Intercomparison of Models for Snowmelt Runoff. Operational Hydrology Report 23, WMO, Geneva.

World Meteorological Organization (WMO), 1992. Simulated Real-Time Intercomparison of Hydrological Models. Operational Hydrology Report 38, WMO, Geneva.

Zarriello, P.J., Ries, K.G., III, 2000. A Precipitation-Runoff Model for Analysis of the Effects of Water Withdrawals on Streamflow, Ipswich River Basin, Massachusetts. USGS Water-Resources Investigations Report 00-4029, 99 p.

Zollweg, J.A., Gburek, W.J., Steenhuis, T.S., 1996. SMoRMod—a GIS-integrated rainfall-runoff model. Trans. ASAE 39, 1299–1307.